Progress In Electromagnetics Research C, Vol. 38, 101–113, 2013

COMPACT DUAL-MODE DOUBLE SQUARE-LOOP RESONATORS FOR WLAN AND WIMAX TRI-BAND FILTER DESIGN

Ji-Chyun Liu[1, *], Feng-Seng Huang[1], Ching-Pin Kuei[1], and Chin-Yen Liu[2]

[1]Department of Electrical Engineering, Chien Hsin University of Science and Technology, Chung-Li, Tao-yuan 32097, Taiwan, R.O.C.

[2]Department of Electronic Engineering, Tahwa Institute of Technology, Qionglin, Hsinchu 307, Taiwan, R.O.C.

Abstract—The improved configurations with dual-mode double-square-loop resonators (DMDSLR) for tri-band application are proposed in this paper. Two sets of loops including double-square-loop and G-shaped loop are involved in the resonators. The resonant frequency equations related to DMDSLR geometries are introduced for simply designing tri-band bandpass filter (BPF). Resonant frequencies and transmission zeroes can be controlled by tuning the perimeter ratio of the square rings and the couples. To obtain lower insertion loss, higher out-of-band rejection level, wider bandwidth of tri-band, and compact applications, the miniaturized DMDSLR structure is designed. The effective design procedure is provided. The proposed filter is successfully simulated and measured. It can be applied to WLAN (2.45, 5.20 and 5.80 GHz) and WiMAX (3.50 GHz) systems.

1. INTRODUCTION

The increasing demand for multi-band applications has required a single wireless transceiver to support multi-band operations. The multi-band BPFs play an important role in a multi-band transceiver, such as dual-band [1, 2], tri-band [3–21] and quad-band [22–29] filters.

Recently, a new excitation for DMDSLR with CPW was proposed for dual-band applications [1]. The square ring resonators with back-to-back and concentric configurations were presented. Due to the effect

Received 20 January 2013, Accepted 19 March 2013, Scheduled 20 March 2013

* Corresponding author: Ji-Chyun Liu (jichyun@uch.edu.tw).

of the CPW input/output structure, performance with low insertion loss and high out-of-band rejection level was achieved. The BPF was used a nested meander loop resonator for dual-band applications [2]. The even/odd-mode method with equivalent circuit was proposed and designed with the split-ring resonator (SRR) to obtain three controllable resonant frequencies [3]. The coupling-matrix design for tri-band filter was presented [4]. The authors developed the frequency transformation for finding the locations of poles and zeros of specific tri-band filters [5]. Moreover, various filters have been realized with the basic SIR and their variety to exhibit tri-band responses [6–11, 13]. Recently, for tri-band filter design, the stub-loaded resonators (SLR) and half-wavelength resonators were presented [14]. And the microstrip and a defeated ground structure (DGS) slot were used [15], and a ring resonator with triple degenerate modes was presented [17].

Applied to WLAN and WiMAX tri-band systems, the open and short stubs loaded crossed resonator were designed [12]. The SLR and DGS resonators were used for applications [16]. Recently, fourth-order tri-band BPF was developed by using square ring loaded resonators [18]. Meantime, the double-square-loop with CPW-fed was proposed [19]. And square ring short stub loaded resonators were presented [20]. Thus, the tri-band BPF for WLAN and WiMAX applications is an interested R&D topic.

Whether the combined quarter-wavelength step impedance resonator (SIR) or assembled half-wavelength SIR was used, the impedance ratio computation and tuning the stub were needed [7–12]. For SLR filter, the stub length was tuned for the desired responses [12, 14–16]. On the other hand, in [6], three closed-form equations related to the resonant frequencies of the tri-band were deduced for simple design. Similarly, in [19] and [23], four simple equations related to the perimeters of the concentric rings were approximated for the multi-band design.

Based on [19] and [23], this paper proposes a novel way with the resonant frequency equations related to DMDSLR geometries for simply designing tri-band BPF. Two types of DMDSLR including DMDSLR and miniaturized DMDSLR are presented for application. The compact filter can be applied to WLAN (2.45, 5.20 and 5.80 GHz) and WiMAX (3.50 GHz) tri-band systems. Tuning the perimeter ratios of the rings and the couples presents the controllable resonant frequencies. For excitation of DMDSLR, the filter is fed by an improved CPW-fed line. The improved T-couple line consists of a feed line and the asymmetric branches. In addition, by using SIR and square perturbations, the novel dual-mode DMDSLR is proposed. The simulation and measurement results, including frequency responses

and current distributions, are presented to analyze the tri-band characteristic The previous filters at the same design frequency of WLAN and WiMAX system are compared.

2. DESIGN OF IMPROVED DMDSLR TRI-BAND FILTER

The perimeters of the square loops are related to the guided wavelength at corresponding resonant frequencies basically. The modified DMDSLR filter employs two sets of the loops to present the dual-band in Figure 1 at first. Then the square loop is designed to operate at the first and third resonated frequencies and the G-shaped loop is employed at the second and fourth resonated frequencies. By using the third and fourth resonated frequencies to form an operating band, a wide pass-band is obtained. Thus, the resonant frequencies of the four resonators can be approximately expressed as [19, 23, 30]:

$$f_1 = \frac{c}{[2(L_1 + L_2) + L_3]\sqrt{\varepsilon_{eff}}} \tag{1}$$

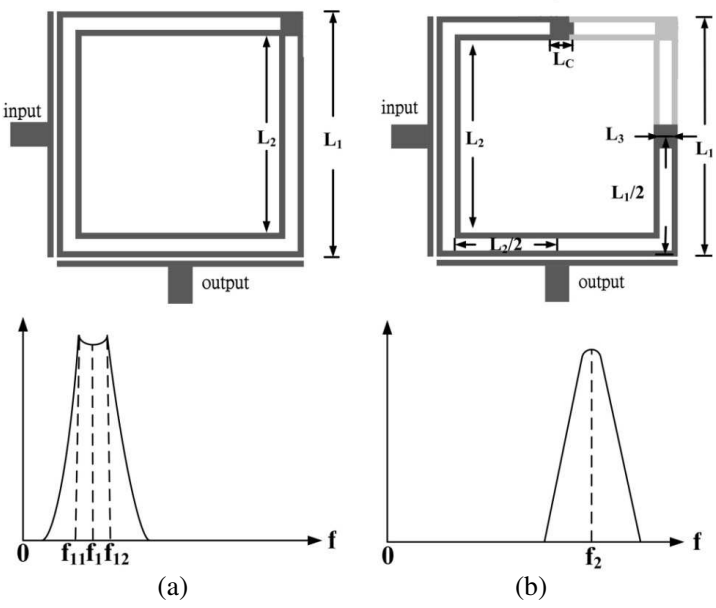

Figure 1. Dual-band configurations. (a) Square loop for band I, and (b) G-shaped loop for band II.

$$f_2 = \frac{2c}{[3(L_1 + L_2) + L_c + 2L_3]\sqrt{\varepsilon_{eff}}} \quad (2)$$

$$f_{3a} = \frac{c}{[(L_1 + L_2) + L_3]\sqrt{\varepsilon_{eff}}} \quad (3)$$

$$f_{3b} = \frac{4c}{[3(L_1 + L_2) + L_c + 2L_3]\sqrt{\varepsilon_{eff}}} \quad (4)$$

where c is the speed of light in free space. L_1 and L_2 denote the side lengths of the two square loops, and L_3 and L_C are the couples between the square loops and ε_{eff} represents the effective permittivity of the substrates.

The square loops related to the dual side-length (L_1 and L_2) decides the resonant frequencies f_a and f_{3a}, and the G-shaped loop related to the folded loop represents the resonant frequencies f_2 and f_{3b} shown in Figures 1(a) and (b). And, the Equations (1) to (4) show that various frequencies of the tri-band can be obtained by adjusting the side-length ratio L_1/L_2 and the couples L_3 and L_C even when its perimeters of the square loops and the couples are given. Thus the resonated frequencies can be determined by choosing a suitable combination of the side-length ratio and the couples of the DMDSLR filter. For excitation of tri-band responses, the square loops are fed by the T-couples.

The simulations for DMDSLR are achieved with IE3D [31]. The Roger-3003 substrate with dielectric constant $\varepsilon_r = 3.0$, loss tangent $\tan\delta = 0.0013$ and thickness $h = 1.57\,\text{mm}$ is used. For the $50\,\Omega$ line, the width is 1.45 mm, length is 4.25 mm, effective dielectric constant $\varepsilon_{eff} = 2.28$, and guided wavelength $\lambda_g = 80\,\text{mm}$, 55 mm and 40 mm for the frequencies $f_0 = 2.4\,\text{GHz}$, 3.5 GHz and 5.8 GHz respectively.

The proposed DMDSLR configuration is shown in Figure 2. For excitation of tri-band responses, the square rings are fed by an improved T-couple. The improved T-couple consists of a feed-line and the asymmetric branches shown in Figure 2. By adjusting the length of the branches, the tri-band responses can be obtained. Due to dual-mode, the bandwidth of each band can be obtained by tuning the perturbation (P_1). The width of $50\,\Omega$ line is given by W_1, and the length is given by L_4. Impedance matching can be improved by adjusting gap width W_2. Physical dimensions are stated: $L_1 = 22.5\,\text{mm}$, $L_2 = 17.1\,\text{mm}$, $L_3 = 6.88\,\text{mm}$, $L_4 = 11.2\,\text{mm}$, $L_5 = 0.75\,\text{mm}$, $L_6 = 3.0\,\text{mm}$, $L_C = 2.77\,\text{mm}$, $W_1 = 2.53\,\text{mm}$, $W_2 = 0.25\,\text{mm}$, $W_3 = 0.7\,\text{mm}$. $W_4 = 1.3\,\text{mm}$, $W_5 = 1.07\,\text{mm}$, $W_6 = 1.15\,\text{mm}$, $W_7 = 0.6\,\text{mm}$, $P_1 = 4.35\,\text{mm}$, and $g_1 = 0.2\,\text{mm}$.

2.1. Frequency Responses

The proposed tri-band BPF is simulated and measured with S_{21} and S_{11} frequency responses in Figure 3. Clearly, the simulated and

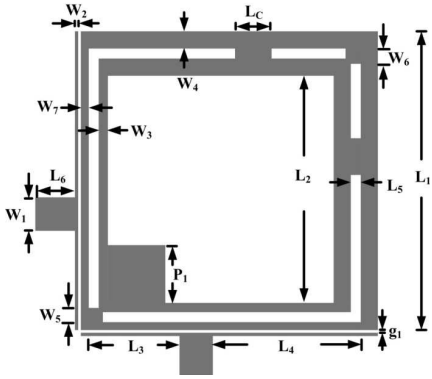

Figure 2. Configuration of DMDSLR.

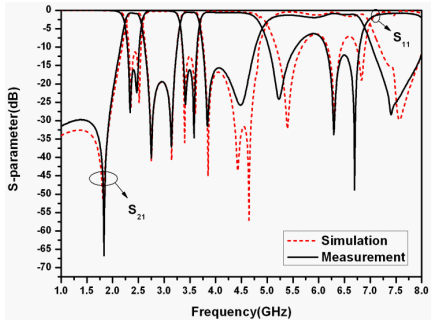

Figure 3. Frequency responses of DMDSLR filter.

Table 1. Results of DMDSLR response.

	DMDSLR		
	Band I	Band II	Band III
Frequencies (GHz)	2.4	3.52	5.85
−3 dB BW (MHz)	324	341	1863
Fractional BW (%)	13.5	9.6	31.8
Maximum insertion loss (dB)	−0.67	−0.48	−0.8
Mode resonances (GHz)	2.3/2.5	3.4/3.6	5.2/6.3/6.7
Transmission zero level (dB)	−70.4/−39.4	−36.5/−31.7	−26.5/−24.9
Calculation (GHz)	2.49	3.4	5.72
Tolerance (%)	3.6	3.4	2.2
	Miniaturized DMDSLR		
	Band I	Band II	Band III
Frequencies (GHz)	2.41	3.57	5.81
−3 dB BW (MHz)	245	367	1426
Fractional BW (%)	10.1	10.1	24.5
Maximum insertion loss (dB)	−0.69	−0.41	−0.86
Mode resonances (GHz)	2.4/2.45	3.5/3.6	5.3/6.2/6.5
Transmission zero level (dB)	−66.2/−48.3	−42.4/−34.4	−34.4/−24.2
Calculation (GHz)	2.42	3.45	5.53
Tolerance (%)	0.4	3.4	4.8

measured results have good agreement. The dual-mode behaviors are presented in each band. All the tri-band responses at 2.42, 3.51 and 5.81 GHz frequencies are listed in Table 1. The lower insertion loss and higher out-of-band rejection level and wider band of the responses are obtained and it is suitable for tri-band applications. Calculation by (1) to (4), the tolerances (less than 10%) related to the measurements are also listed.

2.2. Current Distributions

Figures 4(a), (b) and (c) present the surface current distributions of DMDSLR filter in each band of the tri-band. In the central configurations of Figures 4(a) and (c), the distributions are presented with even and odd modes in band I (2.35 and 2.52 GHz) around the two square loops respectively. In the central parts of Figures 4(b) and (d) are the distributions of even and odd modes in band II (3.39 and 3.6 GHz) around the G-shaped loops respectively. There are three resonances in band III (5.39, 6.31 and 6.82 GHz) exist in the DMDSLR. In both sides of Figures 4(a) to (c), these are distributions of two transmissions.

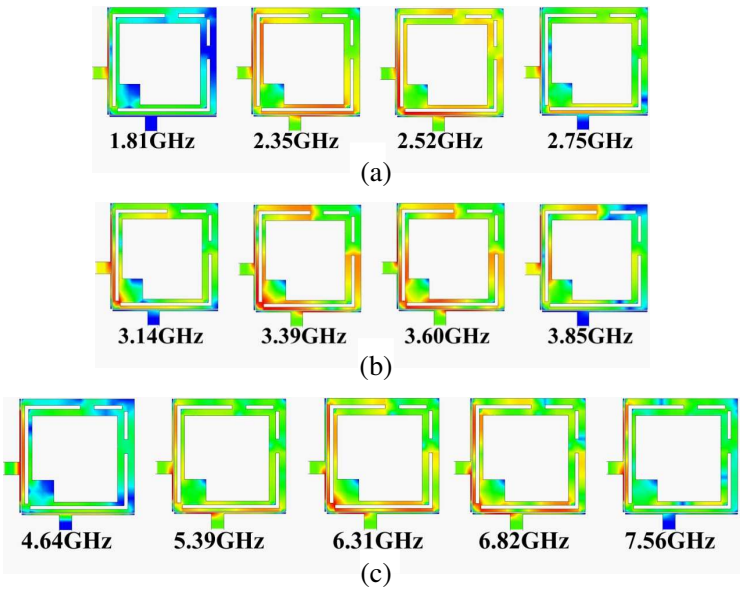

Figure 4. Current distributions of DMDSLR filter. (a) Band I, (b) band II, and (c) band III.

2.3. Design Procedure

For simply and accuracy design, this paper proposes a systematic design procedure by using the variations of side-length ratio of the tri-band filter. Since the perimeters of the square loops determine the first resonated frequency, and the perimeters of the G-shaped loops determine the second resonated frequency mainly, thus, the Equations (1) and (2) show two frequencies can be obtained by adjusting the side-length ratio L_1/L_2 and the couple L_3 at first. Then the BW of each band related to the couple (L_3) and perturbation (P_1) can be obtained by tuning. Both resonated frequencies and bandwidth in each band are controllable. Second, the third band is the periodicity of the first and second resonated frequencies basically. The Equations (3) and (4) show that the lower/higher frequencies of the third band. The lower/higher frequencies can be obtained by adjusting the side-length ratio and the couple. The BW of the third band also related to the couple and perturbation can be obtained by tuning. Finally, the response is obtained by tuning the improved T-couple line.In practical design procedure, we can choose appropriate values for those parameters and by tuning to obtain the desired responses.

3. DESIGN OF MINIATURIZED DMDSLR TRI-BAND FILTER

For miniaturization [2], the meander-line DMDSLR is designed in Figure 5 and the physical dimensions are stated: Tri-band DMDSLR

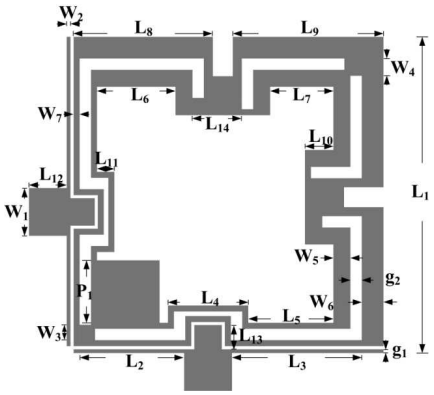

Figure 5. Miniaturized DMDSLR configuration.

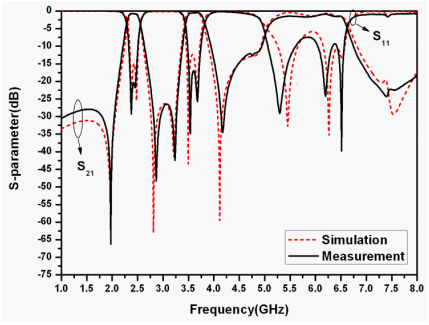

Figure 6. Frequency responses of miniaturized DMDSLR.

with $L_1 = 21\,\text{mm}$, $L_2 = 6.925\,\text{mm}$, $L_3 = 8.6\,\text{mm}$, $L_4 = 5.325\,\text{mm}$, $L_5 = 5.645\,\text{mm}$, $L_6 = 5.2\,\text{mm}$, $L_7 = 4.19\,\text{mm}$, $L_8 = 9.23\,\text{mm}$, $L_9 = 9.99\,\text{mm}$, $L_{10} = 1.885\,\text{mm}$, $L_{11} = 1.15\,\text{mm}$, $L_{12} = 2.5\,\text{mm}$, $L_{13} = 1.61\,\text{mm}$, $L_{14} = 3.27\,\text{mm}$, $W_1 = 3.175\,\text{mm}$, $W_2 = 0.25\,\text{mm}$, $W_3 = 1.02\,\text{mm}$, $W_4 = 1.15\,\text{mm}$, $W_5 = 1.13\,\text{mm}$, $W_6 = 1.44\,\text{mm}$, $W_7 = 0.4\,\text{mm}$, $g_1 = 0.21\,\text{mm}$, $g_2 = 0.75\,\text{mm}$, and $P_1 = 4.15\,\text{mm}$.

3.1. Frequency Responses

The proposed tri-band BPF is simulated and measured with S_{21} and S_{11} frequency responses in Figure 6. Clearly, the simulated and measured results have good agreement. The dual-mode behaviors are presented in each band. All the tri-band responses are also listed in Table 1. Similarly, the lower insertion loss and higher out-of-band rejection level and wider band of the responses are obtained and it is suitable for tri-band applications. Calculation by (1) to (4), the tolerances (less than 10%) related to the measurements are also listed.

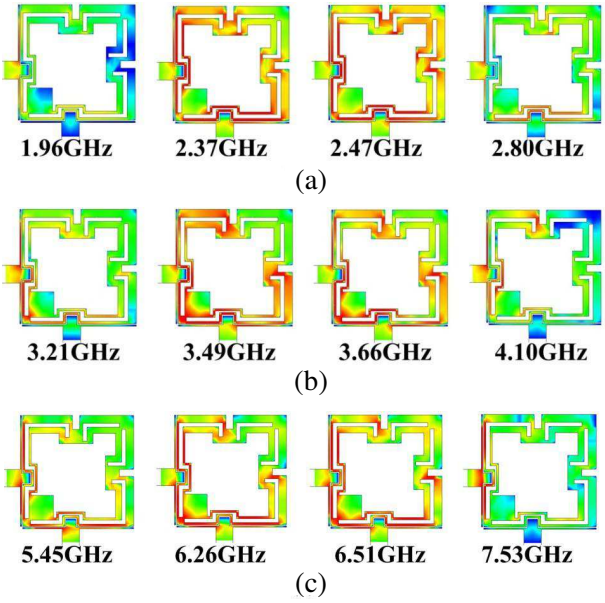

Figure 7. Current distributions of miniaturized DMDSLR filter. (a) Band I, (b) band II, and (c) band III.

3.2. Current Distributions

Figures 7(a) to (c) present the surface current distributions. All the square loops exhibit the identical surface current distributions according to multiple resonance (2.37 and 2.47 GHz), (3.49 and 3.66 GHz), (5.45, 6.26 and 6.51 GHz) respectively. The transmission zero (1.96 and 2.8 GHz), (3.21 and 4.1 GHz), (4.1 and 7.53 GHz) are represented with attenuation (blue) in output port. The photograph is presented in Figure 8. The size reduction with 13% is obtained.

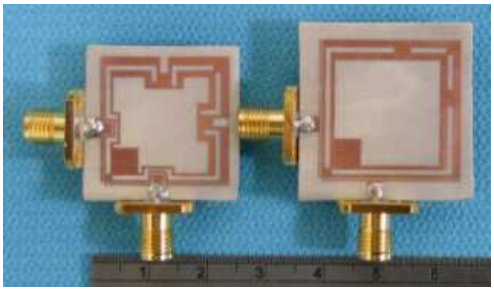

Figure 8. The photograph of the proposed filters.

3.3. Comparison

Compared with the filters at the same design frequency of WLAN and WiMAX system [12, 16, 18–20], the performance of the six filters are listed in Table 2. The four filters cover the required bandwidths for WLAN band (2.4–2.48 GHz and 5.15–5.35 GHz) and WiMAX (3.4–3.6 GHz) applications [12, 16, 18, 20]. The proposed filter in this paper can significantly extends the 5.2 GHz response up to 5.8 GHz (Fractional BW = 24.5%). It covers the complete WLAN band (2.4–2.48 GHz, 5.15–5.35 GHz, and 5.725–5.825 GHz). The frequency response and bandwidth in the third band are improved in the proposed filter. The return loss within the pass-band is better than 20 dB and the maximum insertion losses are 0.69, 0.41, and 0.86 dB in the proposed filter. In contrast to the losses of 1.88, 1.65 and 0.93 dB, and the FBW = 5.2 and 6.9% in band I and II [19], we have better characteristics. The maximum attenuation between the first and second pass-band is 48.3 dB. The compact size is $23.5 \times 23.5 \times 1.57\,\text{mm}^3$ which is smaller the work of [19].

Table 2. Six tri-band filters for comparison.

Tri-band filters	Ref. [12]	Ref. [16]	Ref. [18]
Frequencies (GHz)	2.4, 3.5, and 5.2	2.44, 3.53, and 5.26	2.4, 3.5, and 5.2
-3 dB BW (MHz)	180, 410, and 210	300, 220, and 170	280, 260 and 160
Fractional BW (%)	7.5, 11.7, and 4.03	12.3, 6.2, and 3.3	8.6, 7.8, and 4.9
Maximum insertion loss (dB)	1.4, 1.1, and 1.7	0.9, 1.7, and 2.1	1.57, 1.6, and 1.77
Transmission zero level (dB)	50, 43, 46, and 35	32, 14, 18, and 27	30.2, 45, and 48
Size (mm^3)	$17.1 \times 17.4 \times 0.8$	$32.0 \times 39.5 \times 2.7$	$48.9 \times 37.8 \times 1.0$
Tri-band filters	Ref. [19]	Ref. [20]	This filter
Frequencies (GHz)	2.48, 3.49 and 5.2/5.8	2.4, 3.5, and 5.2	2.41, 3.57, and 5.2/5.8
-3 dB BW (MHz)	130, 240 and 1820	130, 140 and 210	245, 367, and 1426
Fractional BW (%)	5.2, 6.9 and 36.6	5, 3.2, and 4.2	10.1, 10.1, and 24.5
Maximum insertion loss (dB)	1.88, 1.65 and 0.93	1.2, 1.1, and 1.5	0.69, 0.41, and 0.86
Transmission zero level (dB)	48.3, 51.7, 36.9, and 22.6	55, 46, 45, 47, 46, 42, 35 and 32	66.2, 48.3, 42.4, 34.4, and 24.2
Size (mm^3)	$23.5 \times 23.5 \times 1.57$	$48.9 \times 37.8 \times 1.0$	$28 \times 28 \times 1.57$

4. CONCLUSIONS

The DMDSLR structure and resonant frequency equations for tri-band BPF provide a viable alternative to current multi-band filter design techniques. Based on the inherent high-Q characteristics of the ring resonators, it is found that the miniaturized DMDSLR filter can successfully present good tri-band pass-band performance, high stop-band rejection and deep transmission zeros between pass-bands. The resonant frequency equations and design procedure are available and useful for simply designing tri-band BPF. Tuning the perimeter ratios of the loops and couples provides four controllable resonant frequencies. The BW of each band can be obtained by tuning the couple and perturbation. Transmission zeros can be obtained by tuning the T-couples.

The proposed compact filter has three good response bandwidths (S_{11} better than 10 dB) of 245 MHz (about 10.1% centered at 2.41 GHz), 367 MHz (about 10.1% centered at 3.57 GHz) and 1426 MHz (about 24.5% centered at 5.81 GHz), which make it easily cover the required bandwidths for WLAN band (2.4–2.48 GHz, 5.15–5.35 GHz, and 5.725–5.825 GHz) and WiMAX (3.4–3.6 GHz) applications. The compact size is $23.5 \times 23.5 \times 1.57\,\text{mm}^3$.

REFERENCES

1. Zhang, X. Y. and Q. Xue, "Novel dual-mode dual-band filters using coplanar-waveguide-fed ring resonators," *IEEE Trans. Microw. Theory Tech.*, Vol. 55, No. 10, 2183–2190, 2007.
2. Dai, X. W., C. H. Liang, and Z. X. Chen, "Novel dual-mode dual-band bandpass filter using nested microstrip meander loop resonators," *Microwave Opt. Technol. Lett.*, Vol. 50, No. 3, 836–838, Mar. 2008.
3. Zhao, H. and T. J. Cui, "Novel triple-mode resonators using split-ring resonator," *Microwave Opt. Technol. Lett.*, Vol. 49, No. 12, 2918–2922, 2007.
4. Mokhtaari, M., J. Bomemana, K. Rambabu, and S. Amari, "Coupling matrix design of dual and triple passband filters," *IEEE Trans. Microw. Theory Tech.*, Vol. 54, No. 11, 3940–3945, 2006.
5. Lee, J. and K. Sarabandi, "Design of triple-passband microwave filters using frequency transformations," *IEEE Trans. Microw. Theory Tech.*, Vol. 56, No. 1, 187–193, 2008.
6. Chen, F. C., Q. X. Chu, and Z. H. Tu, "Tri-band bandpass filter

using stub loaded resonators," *Electronics Letters*, Vol. 44, No. 12, 747–749, 2008.

7. Chen, C. F., T. Y. Huang, and R. B. Wu, "Design of dual- and triple-passband filters using alternately cascaded multiband resonators," *IEEE Trans. Microw. Theory Tech.*, Vol. 54, No. 9, 3550–3558, 2006.
8. Lee, C. H., C. I. G. Hsu, and H. K. Jhuang, "Design of a new tri-band microstrip BPF using combined quarter-wavelength SIRs," *IEEE Microw. Wireless Compon. Lett.*, Vol. 16, No. 11, 594–596, 2006.
9. Chu, Q. X. and X. M. Lin, "Advanced triple-band bandpass filter using tri-section SIR," *Electronics Letters*, Vol. 44, No. 4, 295–296, 2008.
10. Hsu, C. I. G., C. H. Lee, and Y. H. Hsieh, "Tri-band bandpass filter with sharp passband skirts designed using tri-section SIRs," *IEEE Trans. Microw. Theory Tech.*, Vol. 18, No. 1, 19–21, 2008.
11. Chen, F. C. and Q. X. Chu, "Design of compact tri-band bandpass filters using assembled resonators," *IEEE Trans. Microw. Theory Tech.*, Vol. 57, No. 1, 165–171, 2009.
12. Chu, Q. X., F. C. Chen, Z. Tu, and H. Wang, "A novel crossed resonator and its applications to bandpass filters," *IEEE Trans. Microw. Theory Tech.*, Vol. 57, No. 7, 1753–1759, 2009.
13. Chen, B. J., T. M. Shen, and R. B. Wu, "Design of tri-band filters with improved band allocation," *IEEE Trans. Microw. Theory Tech.*, Vol. 57, No. 7, 1790–1797, 2009.
14. Zhang, X. Y., Q. Xue, and B. J. Hu, "Planar tri-band bandpass filter with compact size," *IEEE Microw. Wireless Compon. Lett.*, Vol. 20, No. 5, 262–264, 2010.
15. Ren, L. Y., "Tri-band bandpass filters based on dual-plane microstrip/DGS slot structure," *IEEE Microw. Wireless Compon. Lett.*, Vol. 20, No. 8, 429–431, 2010.
16. Lai, X., C. H. Liang, H. Di, and B. Wu, "Design of tri-band filter based on stubloaded resonator and DGS resonator," *IEEE Microw. Wireless Compon. Lett.*, Vol. 20, No. 5, 265–267, 2010.
17. Luo, S., L. Zhu, and S. Sun, "Compact dual-mode triple-band bandpass filters using three pairs of degenerate modes in a ring resonator," *IEEE Trans. Microw. Theory Tech.*, Vol. 59, No. 5, 1222–1229, 2011.
18. Chen, J. Z., N. Wang, Y. He, and C. H. Liang, "Fourth-order tri-band bandpass filter using square ring loaded resonators," *Electronics Letters*, Vol. 47, No. 15, 858–859, 2011.

19. Liu, C.-Y., B.-H. Zeng, J.-C. Liu, C.-C. Chen, and D.-C. Chang, "Dual-mode CPW-FED double square-loop resonators for WLAN and WiMAX tri-band design," *Progress In Electromagnetics Research C*, Vol. 23, 83–93, 2011.
20. Doan, M. T., W. Q. Che, and W. J. Feng, "Tri-band bandpass filter using square ring short stub loaded resonators," *Electronics Letters*, Vol. 48, No. 2, 106–107, 2012.
21. Chen, W. Y., M. H. Weng, and S. J. Chang, "A new tri-band bandpass filter based on stub-loaded step-impedance resonator," *IEEE Microw. Wireless Compon. Lett.*, Vol. 22, No. 4, 179–181, 2012.
22. Hsu, C. I. G., C. H. Lee, and H. K. Jhuang, "Design of a novel quad-band microstrip BPF using quarter-wavelength stepped-impedance resonators," *Microw. J.*, Vol. 50, No. 2, 102–112, 2007.
23. Liu, J. C., J. W. Wang, B. H. Zeng, and D. C. Chang, "CPW-fed dual-mode double-square-ring resonators for quad-band filters," *IEEE Microw. Wireless Compon. Lett.*, Vol. 20, No. 3, 142–144, 2010.
24. Cheng, C. M. and C. F. Yang, "Develop quad-band (1.57/2.45/3.5/5.2 GHz) bandpass filters on the ceramic substrate," *IEEE Microw. Wireless Compon. Lett.*, Vol. 20, No. 5, 268–270, 2010.
25. Ren, L. Y., "Quad-band bandpass filter based on dual-plane microstrip/DGS slot structure," *Electronics Letters*, Vol. 46, No. 1, 691–692, 2010.
26. Wu, H. W. and R. Y. Yang, "A new quad-band bandpass filter using asymmetric stepped impedance resonators," *IEEE Microw. Wireless Compon. Lett.*, Vol. 21, No. 4, 203–205, 2011.
27. Lin, S. C., "Microstrip dual/quad-band filters with coupled lines and quasi-lumped impedance inverters based on parallel-path transmission," *IEEE Trans. Microw. Theory Tech.*, Vol. 49, No. 8, 1937–1946, 2011.
28. Wu, J. Y. and W. H. Tu, "Design of quad-band bandpass filter with multiple transmission zeros," *Electronics Letters*, Vol. 47, No. 8, 502–503, 2011.
29. Xu, J., C. Miao, L. Cui, Y. X. Ji, and W. Wu, "Compact high isolation quad-band bandpass filter using quad-mode resonator," *Electronics Letters*, Vol. 48, No. 1, 28–30, 2012.
30. Chang, K. and L. H. Hsieh, *Microwave Ring Circuits and Related Structures*, John Wiley & Sons, Inc., New Jersey, 2004.
31. Zeland Software Inc., IE3D version 10.0, Jan. 2005.